J. Fluid Mech. (1994), *vol.* 281, *pp.* 293–311

Sound radiation from a cylindrical duct. Part 1. Ray structure of the duct modes and of the external field

By C. J. CHAPMAN †

Department of Applied Mathematics and Theoretical Physics, University of Cambridge, Silver Street, Cambridge CB3 9EW, UK

(Received 18 April 1994 and in revised form 18 July 1994)

This paper determines the ray structure of a spinning acoustic mode propagating inside a semi-infinite circular cylindrical duct, and thereby determines the ray structure of the field radiated from the end of the duct. Inside the duct, but outside of a caustic cylindrical surface, the rays are piecewise linear helices; on striking the rim of the end-face of the duct, these rays produce 'Keller cones' of diffracted rays. The cones determine the structure of the radiated field: for example, no rays penetrate two cone-shaped far-field quiet zones centred on the duct axis; two rays pass through each point in a forward loud zone; and one ray passes through each point in a rearward loud zone. The two rays through each point in the forward loud zone interfere to produce an oscillatory directivity pattern. One quarter of the rays on each cone point back inside the duct and produce the reflected field. Thus the rim of the end-face of the duct acts as a 'ring source', in which the radiated and reflected fields have their origin. Every propagating duct mode determines a polar angle and an azimuthal angle; these are taken as parameters specifying the mode and are used to calculate the positions and angles of all the rays. The mathematical method on which the paper is based is Debye's approximation for the Bessel function which appears in the expression for the duct modes; the approximation shows also that the duct contains a region of smooth helical rays on which the field consists of inhomogeneous waves: this region is the inner cylinder, lying inside the annulus of piecewise linear helical rays. The results of the paper are very promising for the application of Keller's geometrical theory of diffraction to detailed calculations of the sound radiated from aeroengine ducts. An alternative description of the field, using Cargill's meridional rays, is summarized.

1. Introduction

A topic of long-standing importance in research work on the noise produced by turbofan aeroengines is the effect of the duct on the sound radiated by the fan. Tyler & Sofrin (1962) set the scene for a large amount of published work in this area in the 1960's and 1970's, and the subject is now prominent again in noise control work on short-duct multi-blade turbofans. For example, a recent NASA reference publication devotes considerable space to the duct acoustics of aeroengines (Eversman

† Present address: Department of Mathematics, University of Keele, Keele, Staffordshire ST5 5BG, UK.

1991), and the 15th AIAA aeroacoustics conference (Longbeach, California, 1993) included sessions entitled 'Ducted fan noise' and 'Turbomachinery duct propagation and radiation'.

One of the most important effects of an aeroengine duct is that the inlet diffracts the spinning acoustic field propagating forwards inside the duct from the fan; much attention has therefore been paid to the model problem of determining the sound radiated from the end of a semi-infinite hard cylindrical duct of circular cross-section. An exact solution of this problem is available by the Wiener–Hopf technique (Levine & Schwinger 1948; Weinstein 1949, 1969; Lansing 1970; Homicz & Lordi 1975); but because of its complexity, simpler approximate methods have been found of great value by aeroacoustic engineers, and the Kirchhoff approximation, in which an estimated acoustic source strength at the duct face is inserted in a radiation integral, has been more widely used in practice (Tyler & Sofrin 1962; Morfey 1969; Goldstein 1976, pp. 210–212; Rice 1978; Boyd, Kempton & Morfey 1984; A. J. Kempton, A. B. Parry & G. P. Howell 1992, private communication). Unfortunately, the Kirchhoff approximation is accurate only for angles which are not too far from the 'main beam', so that it cannot be relied on for sideways radiation and fails in the rear arc. A natural question, therefore, is whether a method exists which overcomes the limitations of Kirchhoff's method, but does not require the machinery of Wiener–Hopf factorizations and contour integrals.

There is such a method: it is Keller's geometrical theory of diffraction (Keller 1958, 1962). Moreover, the conditions for its validity are easily satisfied in modern turbofans, because the large number of fan blades gives rise to sound of wavelength small compared with the duct radius. Not only does Keller's theory give the sideways and rearward radiation, it deals easily with bell-mouth and scarf inlets, and with arbitrary impedance of the noise-control lining in the duct wall; it is therefore ideal for noise-shielding work (Broadbent 1977; Jones 1977).

Despite the advantages of Keller's method, and its widespread use in many problems of acoustics and electromagnetism, its application to duct acoustics has so far been limited to the calculation of radiation from two-dimensional parallel-plate ducts (e.g. Yee, Felsen & Keller 1968; Boyd *et al.* 1984, equation 4 and appendix 1), and from two-dimensional sectoral-horn ducts (Kinber 1962). The reason for the neglect of such a powerful method for analysing the acoustics of cylindrical ducts appears to be that a complete three-dimensional ray description of cylindrical duct modes is not available in the literature. Since acoustic fields in ducts are nearly always expressed as sums of modes, the decomposition of each mode into its constituent rays is essential if Keller's method is to be added to the repertoire of existing computer codes useful for duct acoustics. Accordingly, the aim of this paper is to show how an arbitrary duct mode may be written as a field of rays, and to deduce the structure of the sound field radiated from the end of the duct; a later paper will use the diffraction coefficient obtained from the exact solution of an appropriate 'canonical problem' to give quantitative detail of the far-field directivity pattern. Although the paper takes as its starting point an explicit expression for the mode, this is not essential: the paper could equally well start with the 'quantum conditions' of Keller & Rubinow (1960).

Previous investigators have determined some aspects of the ray structure of duct modes; in particular, the 'mode ray angle' has been recognised as a fundamental quantity (Weinstein 1949, equation 65, and 1969, equation 15.03; Rice 1978, equations 4 and 9; Rice, Heidmann & Sofrin 1979; Kempton *et al.* 1992, private communication). But two angles, not one, are needed to determine the direction of the rays striking the wall of the duct, because as well as being tilted to the duct axis the rays lie in planes

tilted at an angle to meridional planes. The two angles are noted briefly by Weinstein (1969, problems 3.13 and 4.18) and incorporated into a systematic theory by Rice *et al.* (1979); the present paper calculates them analytically and thereby builds up a complete three-dimensional ray picture, inside the duct and out. Other ray analyses of cylindrical duct problems have been given (e.g. Felsen & Yee 1968; Felsen 1984), but they emphasize localized sources in the duct rather than ray decomposition of individual modes. Weinstein (1969, pp. 166–170) obtained the 'edge-waves' from a cylindrical duct in which the circumferential order of the incident mode is low; but he proceeded by asymptotic analysis of the complicated Wiener–Hopf solution, not by direct use of ray theory.

The reader may find it helpful to inspect the diagrams before proceeding further, as they summarize the geometrical results. The next section presents a detailed analysis of the duct modes and of the ray structure of the radiated field, and the final section contains a discussion of results obtainable from Keller's theory without excessive calculation.

2. Analysis and geometry

2.1. *Notation*

The main result of this paper is that a propagating acoustic mode

$$p = \mathrm{e}^{-\mathrm{i}(\omega t - m\phi - k_x x)} J_m(k_r r) \tag{2.1}$$

in a cylindrical duct of circular cross-section has the helical ray structure shown in figure 1(*a-d*), and produces cones of rays in the external field when it strikes the end of the duct (figure 1*a,b*). Here p is the pressure, t the time, and (r, ϕ, x) a system of cylindrical coordinates aligned with the duct axis; the positive x-direction is out of the duct and will be called forwards. The parameters specifying the mode are its frequency ω, circumferential order m, axial wavenumber k_x, and radial wavenumber k_r. For the moment these will be assumed real and positive, so that the mode is spinning in the direction of increasing ϕ and propagating forwards; m is an integer, to ensure periodicity of 2π in ϕ.

The ray structure in the duct and external field will now be deduced from (2.1) by simple algebraic manipulation, and the field on all the rays in the duct will be obtained in 'free-space' form; calculation of the field on external rays is deferred to a later paper. All angles and lengths will be calculated as functions of the mode parameters. For definiteness, the duct wall at radius $r = a$ is assumed hard, so that $J'_m(k_r a) = 0$, i.e.

$$k_r a = j'_{ms} \qquad (s = 1, 2, \ldots) \quad , \tag{2.2}$$

where s is the radial order of the mode and j'_{ms} is the sth zero of J'_m. Thus k_r can take only a discrete set of values labelled by (m, s), and may be written $k_r^{(ms)}$. Since the pressure field satisfies the wave equation, k_x satisfies $k_x^2 = k^2 - k_r^2$, where $k = \omega/c$ is the free-space wavenumber corresponding to frequency ω, and c is the speed of sound; the mode propagates (i.e. is 'cut on') if k_x is real, and evanesces (i.e. is 'cut off') if k_x is imaginary. In what follows, it is assumed that ka is fixed, and that the mode is cut on; hence $k_r < k$, and m and s are restricted by $j'_{ms} < ka$, so that only finitely many modes are cut on for a given frequency. Hence for given ka there is a maximum cut-on circumferential order m, and for given ka and m there is a maximum cut-on radial order, say $s = s_m = s_m(ka)$. The structure of the non-spinning modes, i.e. modes

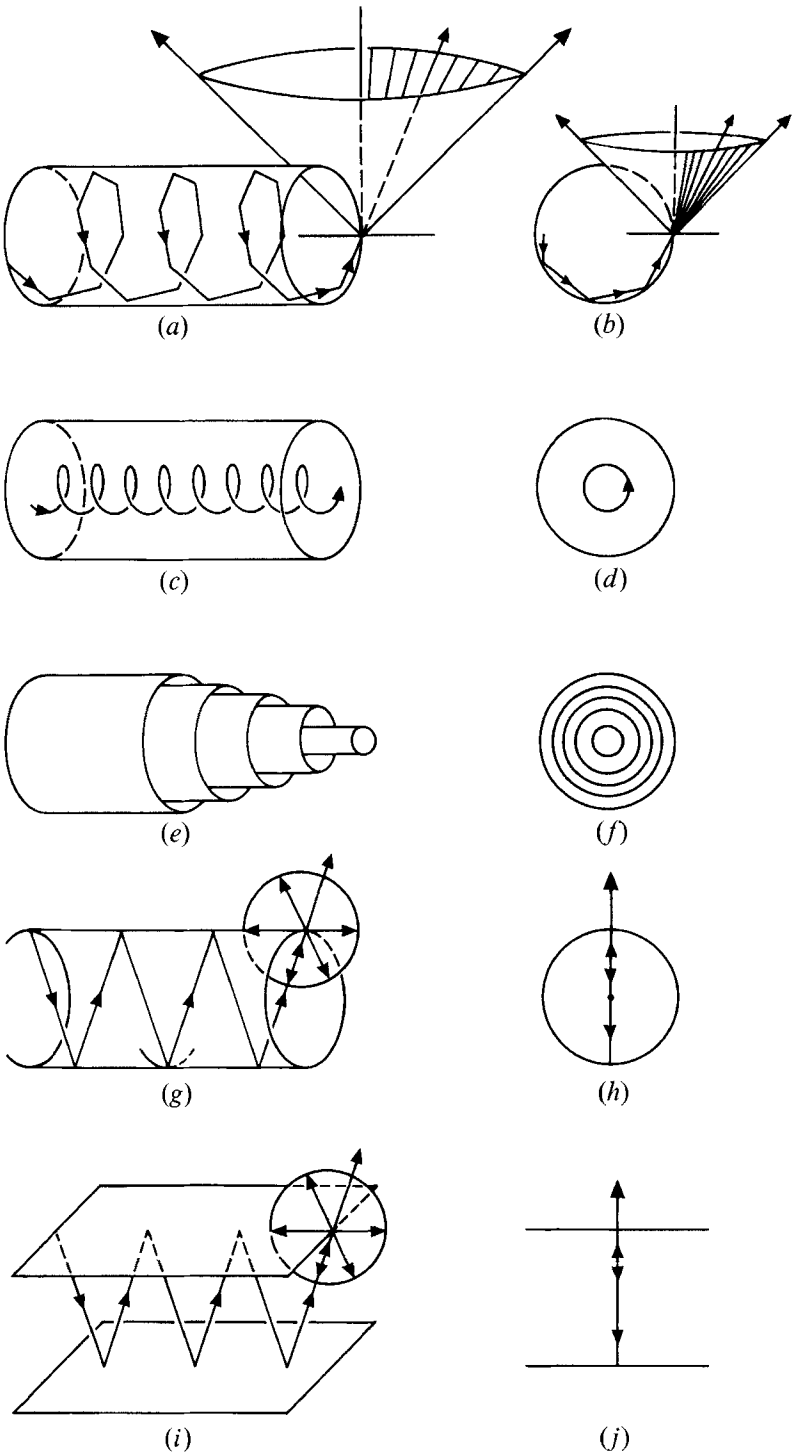

FIGURE 1. For caption see facing page.

for which $m = 0$, may be obtained in an obvious way from the results which follow, but will not be given explicitly.

Since rather a large number of angles and radii will be introduced, it is convenient to present here, for future reference, a systematic set of definitions; figures 1–3 show their geometrical meaning. The starting point is the relation

$$m < j'_{ms} < ka \quad , \tag{2.3}$$

in which the first inequality is a property of Bessel functions, and the second inequality is the cut-on condition just given. Hence angles $\theta_m, \theta_{ms}, \phi_{ms}$ and radii r_m, r_{ms} may be defined by

$$\sin\theta_m = \frac{m}{ka} \quad , \quad \sin\theta_{ms} = \frac{j'_{ms}}{ka} \quad , \quad \sin\phi_{ms} = \frac{m}{j'_{ms}} \tag{2.4a–c}$$

and

$$r_m = a\sin\theta_m \quad , \quad r_{ms} = a\sin\phi_{ms} \quad ; \tag{2.5a, b}$$

then

$$\sin\theta_m = \sin\theta_{ms}\sin\phi_{ms} \quad , \tag{2.6}$$

$$r_m = r_{ms}\sin\theta_{ms} \quad , \tag{2.7}$$

and

$$r_m < r_{ms} < a \quad . \tag{2.8}$$

The relations

$$\frac{r_m}{a} = \frac{m}{ka} \quad , \quad \frac{r_{ms}}{a} = \frac{m}{ka\sin\theta_{ms}} \quad , \tag{2.9a, b}$$

$$k\sin\theta_{ms} = \frac{m}{r_{ms}} \quad , \quad k\cos\theta_{ms} = \left(k^2 - \frac{m^2}{r_{ms}^2}\right)^{1/2} \tag{2.10a, b}$$

and definitions

$$\psi_m = \frac{\pi}{2} - \theta_m \quad , \quad \beta_{ms} = \frac{\pi}{2} - \phi_{ms} \quad , \tag{2.11a, b}$$

i.e.

$$\cos\psi_m = \sin\theta_m \quad , \quad \cos\beta_{ms} = \sin\phi_{ms} \quad , \tag{2.12a, b}$$

will be found useful; they give

$$(k_x, k_r) = (k\cos\theta_{ms} \ , \ k\sin\theta_{ms}) = \left(k\cos\theta_{ms} \ , \ \frac{m}{r_{ms}}\right) \tag{2.13}$$

and

$$p = \mathrm{e}^{-\mathrm{i}(\omega t - m\phi - kx\cos\theta_{ms})} J_m\left(\frac{mr}{r_{ms}}\right) \quad . \tag{2.14}$$

FIGURE 1. Ray geometry: side-views and end-views. (*a*), (*b*) Piecewise linear helix and its Keller cone. The lines on the cone show the directions of incident rays from the piecewise linear helices of other radial orders at fixed circumferential order. (*c*), (*d*) Smooth helical ray in the inner cylinder. (*e*), (*f*) Cylindrical surfaces at the caustic radii $r_{m1}, r_{m2}, \ldots, r_{ms_m}$ and at the sonic radius r_m. (*g*), (*h*) Non-spinning mode, $m = 0$. Each cone is flattened into a disc of infinite radius, so that all the rays lie in meridional planes. (*i*), (*j*) Two-dimensional parallel-plate duct: similar to (*g*), (*h*), but not to (*a*)–(*d*).

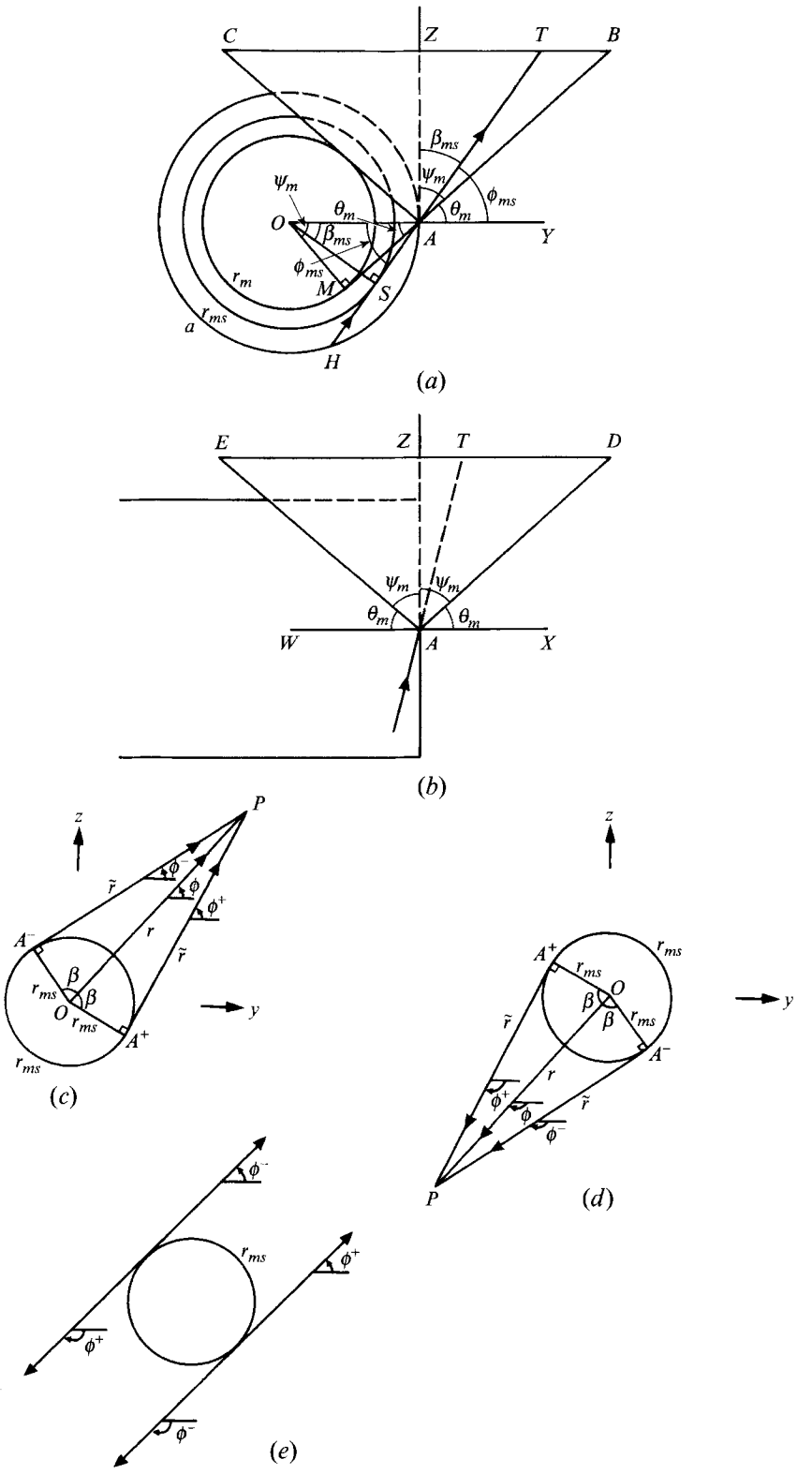

FIGURE 2. For caption see facing page.

Relation (2.10*a*) will often be used to interchange 'k and an angle' with 'm and a radius'.

The above quantities are named as follows: θ_{ms} and ϕ_{ms} are the mode angles, the former being the polar angle and the latter the azimuthal angle; θ_m is the quiet-zone angle, ψ_m the cone angle, β_{ms} the Debye angle at the duct wall, r_m the sonic radius, and r_{ms} the caustic radius. The region $0 \leqslant r \leqslant r_{ms}$ is the inner cylinder, and its surface $r = r_{ms}$ is the caustic cylindrical surface (or 'caustic surface', or 'caustic'); the region $r_{ms} \leqslant r \leqslant a$ is the outer annulus (or 'annulus'); the region $0 \leqslant r \leqslant a$ is the duct; and $r = a$ is the duct wall (or 'wall'). Figure 2(*a,b*) illustrates these quantities. Earlier investigators have called θ_{ms} the mode ray angle (see §1).

The Bessel function in (2.14) oscillates in the annulus $r > r_{ms}$ and decays in the inner cylinder $r < r_{ms}$. Hence it is natural to write J_m in the annulus in terms of the two Hankel functions $H_m^{(1)}$ and $H_m^{(2)}$, and regard the field there as a superposition of two propagating waves; their sum is a field whose variation with r, but not x or ϕ, is that of a standing wave. Within the inner cylinder there is no advantage in decomposing the Bessel function: the exponential decay for $r < r_{ms}$ represents a single inhomogeneous wave. The field in these two regions will now be analysed separately.

2.2. *Outer annulus*

On putting $J_m = \frac{1}{2}(H_m^{(1)} + H_m^{(2)})$, the field (2.14) becomes

$$p = \tfrac{1}{2}(p^+ + p^-) \quad , \tag{2.15}$$

where

$$p^+ = \mathrm{e}^{-\mathrm{i}(\omega t - m\phi - kx\cos\theta_{ms})} H_m^{(1)}\left(\frac{mr}{r_{ms}}\right) \quad , \tag{2.16}$$

and

$$p^- = \mathrm{e}^{-\mathrm{i}(\omega t - m\phi - kx\cos\theta_{ms})} H_m^{(2)}\left(\frac{mr}{r_{ms}}\right) \quad . \tag{2.17}$$

Hence

$$p^\pm \sim \left(\frac{2}{\pi m}\frac{r_{ms}}{\tilde{r}}\right)^{1/2} \mathrm{e}^{-\mathrm{i}\Psi^\pm} \quad , \tag{2.18}$$

where

$$\Psi^\pm = \omega t - m\phi - kx\cos\theta_{ms} \mp \left\{m\left(\frac{\tilde{r}}{r_{ms}} - \beta\right) - \frac{\pi}{4}\right\} \quad , \tag{2.19}$$

and

$$\tilde{r} = (r^2 - r_{ms}^2)^{1/2} \quad , \quad \cos\beta = \frac{r_{ms}}{r} \quad , \quad \tan\beta = \frac{\tilde{r}}{r_{ms}} \quad ; \tag{2.20a–c}$$

FIGURE 2. Definitions of lengths and angles. (*a*), (*b*) Projections of rays and cones: HSA is the last segment of a piecewise linear helix which strikes the rim of the duct at A; the segment continues as AT. In three dimensions, the lines $HSAT$, MAB, AC, AD and AE are all at the cone angle ψ_m to the rim-tangent AZ, and the line AT is at the mode polar angle θ_{ms} to AX; the line $HSAT$ points out of the page in both figures, but the following angles refer to the projections on the page: cone angle $\psi_m = B\hat{A}Z = C\hat{A}Z = D\hat{A}Z = E\hat{A}Z = M\hat{O}A$; quiet-zone angle $\theta_m = B\hat{A}Y = C\hat{A}O = D\hat{A}X = E\hat{A}W = M\hat{A}O$; mode azimuthal angle $\phi_{ms} = S\hat{A}O = T\hat{A}Y$; Debye angle at the wall, $\beta_{ms} = S\hat{O}A$. (*c*), (*d*), (*e*) Offset (or 'annular') polar coordinates $(\tilde{r}, \phi^+)$ and $(\tilde{r}, \phi^-)$, defined for P outside a circle of radius r_{ms}.

see figure 2(*a–d*). In the definition (2.20) of $\tilde{r}$, the argument of the square root is positive, because $r > r_{ms}$ in the outer annulus. The expressions for p^+ and p^- in (2.18) use the Debye approximation to the Bessel functions for 'argument greater than order' (Abramowitz & Stegun 1965, §9.3.3). Although the theory on which the approximation is based requires m to be 'large', a numerical check shows that the approximation remains accurate not merely down to quite small m but in fact down to, and including, $m = 0$. High accuracy at such m is perhaps best regarded as numerical good fortune, since in the absence of realistic error bounds it arises from the numerical evaluation of 'order one' quantities, not from the asymptotic theory itself; this interpretation in no way limits the physical meaning of the approximation, which is that the acoustic field has a ray structure in all regions of space where the Bessel function is well approximated by Debye's formula, whether or not these regions of good agreement have been determined theoretically. Figure 5 in the Appendix compares the exact values of J_m and Y_m with their Debye approximations for $m = 0, 1, 4, 24$. The Appendix also indicates the minor modification needed to the usual form of Debye's approximations to enable them to apply for $m = 0$; they then become identical to the large-argument, fixed-order 'Hankel type' asymptotic approximations to the Bessel functions of order $m = 0$. For all other values of m, the Debye type of asymptotic approximation is quite different from the Hankel type, and numerically is greatly superior to it. Figure 5 shows that the Debye approximation fails only in the 'quarter-wave' on either side of the 'caustic value', i.e. the value at which the argument equals the order; since this remark holds good for all m, Debye's formula may for practical purposes be regarded not so much as a 'large m' approximation, but rather an approximation which fails only in the 'quarter-wave' on either side of the caustic, for any m. As Debye's approximation is the fundamental mathematical tool used in this paper, these remarks are important in determining the paper's scope; for example, r_{ms} has to be very close indeed to a for the ray theory description in the annulus to break down. Therefore the theory applies even for modes which are only just cut on. The author believes that the power of Debye's approximation for, say, $m = 0, 1$, is not widely appreciated.

Expression (2.18) for $p^{\pm}$ is the first term of an asymptotic ray series, in which the phase $\Psi^{\pm}$ satisfies the eikonal equation and higher-order terms satisfy the transport equations. In writing down this ray series, it is essential to scale m with k, so that there is a single large parameter, which may be taken to be k. Terms beyond the first in the series may be found either by solving the transport equations, or, more directly, by using the known expressions for the higher-order terms in Debye's asymptotic series for the Bessel functions.

The phase $\Psi^{\pm}$ defined in (2.19) represents a plane wave on every tangent plane to the caustic cylindrical surface (figure 3), because $\phi \pm \beta$ is constant on the (negative, positive) half-planes comprising a tangent plane (figures 2*c–e* and 3*a*), and because $(x, \tilde{r})$ are ordinary Cartesian coordinates on the tangent plane (except that $\tilde{r}$ is positive by definition). Note that the 'Debye angle' β depends on r; hence the constancy of $\phi \pm \beta$ on half-planes tangent to the particular cylinder $r = r_{ms}$ is a non-trivial property of $\Psi^{\pm}$ which reflects the fact that Debye's approximation is intimately related to a particular ray structure, namely a family of straight lines expressed in polar coordinates. This has been noted before (e.g. Keller 1958, equations 29, 31; Kinber 1962, equation 4; Kravtsov 1967, equation 25).

In order to describe the field in detail on tangent planes to the caustic cylindrical surface, some care is needed with a sign convention, because two tangent planes pass through each point in the annulus, and any one tangent plane consists of two

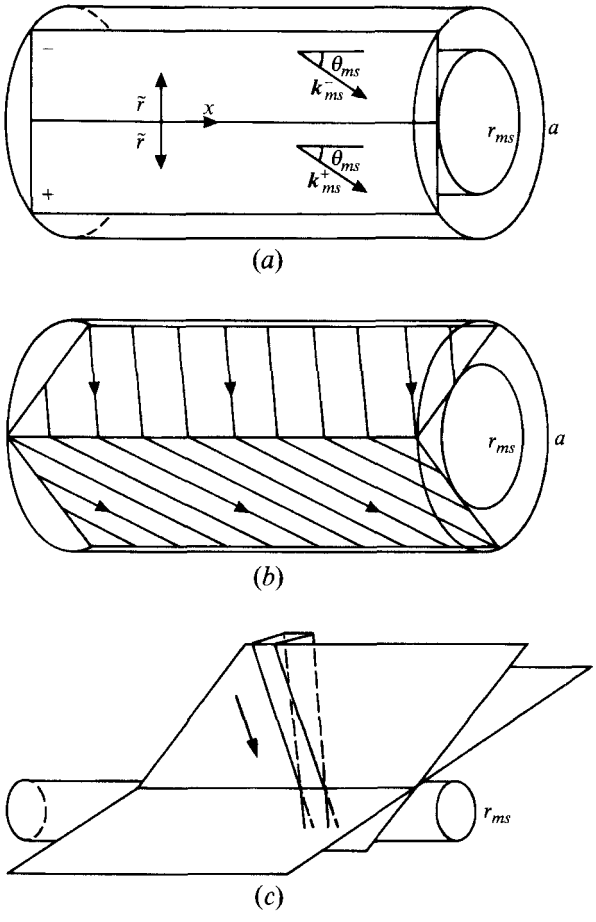

FIGURE 3. Tangent planes to the caustic cylindrical surface. (*a*) Constituent half-planes, and the ray direction $\boldsymbol{k}^{\pm}_{ms}$. (*b*) Reflection at the duct wall. (*c*) A ray tube.

half-planes, one from each of two families. To avoid ambiguity, the variable $\tilde{r}$ will be used to form two systems of annular (or 'offset') polar coordinates $(\tilde{r}, \phi^+)$ and $(\tilde{r}, \phi^-)$, as shown in figure 2(*c–e*). Thus ϕ^+ is constant on one half of a tangent plane, to be called the positive half-plane; as a point moves away from the cylinder at fixed ϕ^+, so ϕ increases, i.e. the direction of rotation about the duct axis is positive. Similarly, ϕ^- is constant on the negative half-plane; as a point moves away at fixed ϕ^-, so ϕ decreases, i.e. the point rotates in the negative direction about the duct axis. Thus ϕ^+ and ϕ^- are positively and negatively offset azimuthal angles; $(\tilde{r}, \phi^+)$ and $(\tilde{r}, \phi^-)$ are positively and negatively offset polar coordinates. One reason for adopting these coordinates is that the relation

$$\phi^{\pm} = \phi \pm \left(\frac{\pi}{2} - \beta\right) \tag{2.21}$$

then holds, modulo 2π, for any point (r, ϕ) in the annulus; thus the two tangent half-planes through a given point can be described analytically without ambiguity. Conversely, the values of ϕ^+ and ϕ^- on the two half-planes comprising a single tangent plane satisfy $\phi^+ - \phi^- = \pi \pmod{2\pi}$, and when $r \to r_{ms}$ so $\tilde{r} \to 0$, $\beta \to 0$, and $\phi^{\pm} \to \phi \pm \pi/2$. At the duct wall $r = a$, the values are $\tilde{r} = a \sin \beta_{ms} = a \cos \phi_{ms}$,

$\beta = \beta_{ms}$, and $\phi_\pm = \phi \pm \phi_{ms}$. Hence at the duct wall, the tangent plane is 'tilted' at an angle ϕ_{ms} to the meridional plane. The offset radius $\tilde{r}$, positive by definition, measures distance from either of the two straight lines in which the two tangent planes through a point in the annulus touch the inner cylinder; $(\tilde{r}, x)$ are rectangular coordinates for either of the two half-planes comprising a tangent plane. Since $\tilde{r}, \phi^+, \phi^-$ and β are defined with respect to a particular caustic cylindrical surface, their values depend not only on r and ϕ but also on m and s through r_{ms} (see (2.20), (2.21)); but m and s will not be incorporated into the notation.

In the above variables, the phase (2.19) becomes

$$\Psi^\pm = \omega t - \boldsymbol{k}^\pm_{ms} \cdot \tilde{\boldsymbol{r}} - m\phi^\pm \pm (m + \tfrac{1}{2})\tfrac{1}{2}\pi \quad , \tag{2.22}$$

where

$$\boldsymbol{k}^\pm_{ms} = k(\cos\theta_{ms} \ , \ \pm \sin\theta_{ms}) \quad , \tag{2.23}$$

$$\tilde{\boldsymbol{r}} = (x, \tilde{r}) \quad , \tag{2.24}$$

and (2.10*a*) has been used. Since $|\boldsymbol{k}^\pm_{ms}| = k = \omega/c$, the phase $\Psi^\pm$ represents waves travelling in straight lines at the speed of sound on half-planes of fixed $\phi^\pm$; cf. the 'free-space waves' of Baxter & Morfey (1986, appendix A) and the numerical results in Rice *et al.* (1979, appendix A and table A1). Note that $\boldsymbol{k}^\pm_{ms}$ points in a single direction θ_{ms} to the duct axis on a whole tangent plane: different values labelled by $\pm$ are needed because an increase in $\tilde{r}$ gives opposite directions on the two half-planes (figure 3*a*). The ray structure is not that of spiral waves in a narrow annulus described by Tyler & Sofrin (1962, figure 9*b*,*c*), Morfey, Sharland & Yeow (1968, figure 10.9*a*), and Wright (1972, figure 3*b*).

The complete field of rays on a tangent plane is shown in figure 3*b*. Two neighbouring tangent planes determine the shape of a ray tube; the tube drawn in figure 3*c* has a fixed width in the axial direction, because the rays within a tangent plane are parallel. In the circumferential direction, the width of the tube is proportional to $\tilde{r}$, which implies that the amplitude of the field in the ray tube must vary as $\tilde{r}^{-1/2}$. The fact that p^+ and p^-, as given by (2.18), do indeed have this variation of amplitude provides a check of the ray theory just developed; and the singularity as $\tilde{r} \to 0$ confirms the presence of the caustic surface at $r = r_{ms}$. A further check is that a caustic surface retards by $\frac{1}{2}\pi$ the phase on each ray passing through it. Now the terms $\omega t - \boldsymbol{k}^\pm_{ms} \cdot \tilde{\boldsymbol{r}}$ in $\Psi^\pm$ are consistent with no phase jump, by the remark after (2.24) that $\boldsymbol{k}^\pm_{ms}$ points in a single direction on the whole tangent plane. Hence the jump arises from the terms $-m\phi^\pm \pm (m + \frac{1}{2})\frac{1}{2}\pi$, and since $\phi^+ - \phi^- = \pi$ for the two half-planes comprising a tangent plane, the phase change in (2.18) is $-(\Psi^+ - \Psi^-) = -\frac{1}{2}\pi$, as expected. In accordance with figure 5 in the Appendix, the ray representation (2.18) in the outer annulus will break down as an approximation to the original field (2.1) only in the thin annulus comprising the quarter-wave next to the caustic.

The two tangent planes containing a straight line in the duct wall are shown in figure 3*b*. Each ray on one tangent plane joins another ray on the next; by symmetry, the composite ray so formed satisfies the 'law of reflection' at the wall: i.e. the incident and reflected rays lie in the same plane and make equal angles with the wall. On following a ray through successive tangent planes and reflections, the resulting composite ray is a piecewise linear helix, in which each segment is at a polar angle θ_{ms} to the duct axis and lies in a plane tilted by an azimuthal angle ϕ_{ms} to the meridional plane through the reflection point on the duct wall; thus on each reflection, the azimuthal angle of the ray increases by $\pi - 2\phi_{ms}$, i.e. $2\beta_{ms}$. This establishes the

ray structure in figure 1*a* and gives the angles in terms of the parameters specifying the mode. The piecewise linear helices are not invariant to translations parallel to the duct axis; i.e. $2\beta_{ms}$ does not divide any integer multiple of 2π, and successive reflection points do not return to an earlier azimuthal angle. The field in the annulus is that of a whispering-gallery mode (Brekhovskikh 1980, pp. 419–421; Weinstein 1969, problem 3.13), though the term might be considered inappropriate for the field inside an aeroengine duct.

2.3. *Inner cylinder*

When $r < r_{ms}$, application of the Debye approximation for 'argument less than order' (Abramowitz & Stegun 1965, §9.3.2) to the Bessel function in (2.14) gives

$$p \sim \left(\frac{1}{2\pi m}\,\frac{r_{ms}}{\tilde{r}}\right)^{1/2} \mathrm{e}^{\Phi - \mathrm{i}\Psi} \tag{2.25}$$

where

$$\Phi = m\left\{\frac{\tilde{r}}{r_{ms}} - \operatorname{sech}^{-1}\left(\frac{r}{r_{ms}}\right)\right\} \quad , \tag{2.26}$$

$$\Psi = \omega t - m\phi - kx\cos\theta_{ms} \quad , \tag{2.27}$$

and now

$$\tilde{r} = (r_{ms}^2 - r^2)^{1/2} \quad . \tag{2.28}$$

Note that the argument of the square root is positive, because $r < r_{ms}$ in the inner cylinder; compare the definition (2.20) of $\tilde{r}$ for $r > r_{ms}$, i.e. in the outer annulus. In all cases, $\tilde{r}$ is positive by definition. The notation

$$\frac{1}{\hat{r}^2} = \frac{1}{r^2} - \frac{1}{r_{ms}^2} \quad , \tag{2.29}$$

i.e.

$$\frac{r}{\hat{r}} = \frac{\tilde{r}}{r_{ms}} \quad , \tag{2.30}$$

is convenient; it gives

$$\frac{\partial\Phi}{\partial r} = \frac{m}{\hat{r}} \quad , \quad \left(\frac{1}{r}\,\frac{\partial\Psi}{\partial\phi} \, , \quad \frac{\partial\Psi}{\partial x}\right) = \left(-\frac{m}{r} \, , \quad -k\cos\theta_{ms}\right) \quad , \tag{2.31a,b}$$

$$|\nabla\Phi|^2 = \frac{m^2}{\hat{r}^2} \quad , \quad |\nabla\Psi|^2 = k^2 + \frac{m^2}{\hat{r}^2} \quad , \tag{2.32a,b}$$

$$|\nabla\Phi|^2 - |\nabla\Psi|^2 = -k^2 \quad , \quad \nabla\Phi\cdot\nabla\Psi = 0, \tag{2.33a,b}$$

which form the basis of what follows. The reason for defining a third radial coordinate $\hat{r}$, in addition to r and $\tilde{r}$, is that $\hat{r}$ occurs naturally in equations (2.31)–(2.34) describing the wave motion in the inner cylinder. As r varies from 0 to r_{ms}, so $\hat{r}$ varies from 0 to ∞; when $r \to 0$, so $\Phi \to -\infty$; and when $r \to r_{ms}$ from below, Φ becomes proportional to $-m(r_{ms} - r)^{3/2}$.

Equations (2.33) express the fact that the field p given by (2.25) is locally an inhomogeneous plane wave (Brekhovskikh 1980, pp. 3–5): the wave propagates in the direction $-\nabla\Psi$ with phase speed $\omega/|\nabla\Psi|$, always less than c by (2.33*a*), and decays exponentially in the transverse direction $-\nabla\Phi$ at a gradient proportional to $\mathrm{e}^{\Phi}|\nabla\Phi|$, i.e. with logarithmic decrement $|\nabla\Phi|$; the other term $\tilde{r}^{-1/2}$ in (2.25) is slowly varying.

A noteworthy feature of a field of inhomogeneous waves of the type (2.25) is that Φ and Ψ can be arbitrary functions of position, so long as they satisfy (2.33) with a constant value of k; recall that $k = \omega/c$, and the speed of sound c is assumed uniform. Thus the phase speed $\omega/|\nabla\Psi|$ depends on position; in effect, the rays are refracted and can be arbitrary curves. This explains why pressure fields satisfying the wave equation with uniform sound speed can travel on rays which are not straight lines. By (2.33*a*), the greater the amount by which the phase speed falls short of c, the greater the rate of exponential decay in the transverse direction. If (2.31)–(2.32) were to be used as the basis for an asymptotic ray series, m would be scaled with k, as noted in §2.2; it would also be customary to scale Φ and Ψ with k so that k appears explicitly in the phase term.

A systematic theory has been developed for ray-tracing of inhomogeneous waves (e.g. Choudhary & Felsen 1974), and the corresponding fields have been related to complex rays (Keller 1958; Kravtsov 1967; Wang & Deschamps 1974). But this theory is not needed here, because the direction of $\nabla\Psi$, from (2.27) and (2.31*b*), implies at once that the rays are helices; on a cylindrical surface of radius r, the helical angle $\theta_{ms}^{(r)}$ and propagation speed $c_{ms}^{(r)}$ are given by

$$\tan\theta_{ms}^{(r)} = \frac{m}{kr\cos\theta_{ms}}, \quad c_{ms}^{(r)} = c\left\{1+\left(\frac{m}{k\hat{r}}\right)^2\right\}^{-1/2}. \tag{2.34a,b}$$

The angle and phase speed tend to θ_{ms} and c as $r \to r_{ms}$ from below, because $m/(kr_{ms}) = \sin\theta_{ms}$, and $\hat{r} \to \infty$. Hence the smooth helical rays in the inner cylinder match smoothly onto the piecewise linear rays in the outer annulus: both direction and phase speed are continuous as the caustic surface $r = r_{ms}$ is crossed. But the breakdown of the Debye approximation (2.25) near this surface must be remembered; figure 5 in the Appendix shows that the excluded annulus just inside the surface $r = r_{ms}$ has approximately the same thickness as the excluded annulus just outside the surface; hence the total thickness, in the ray direction, of the excluded annulus surrounding $r = r_{ms}$ is that of half a wave.

The ray angle $\theta_{ms}^{(r)}$ increases as r decreases, and the axial distance travelled by a ray in one revolution about the axis is $(2\pi kr^2/m)\cos\theta_{ms}$. Hence the propagation of the field on rays does not correspond to a helical motion of a solid cylinder; for example, the rays near the duct axis are almost circumferential in direction, as noted by Rice *et al.* (1979, appendix A).

2.4. *The ring source and the Keller cones*

Each point on the rim of the end-face of the duct is struck by a piecewise linear ray from the outer annulus inside the duct, and becomes the vertex of a Keller cone of diffracted rays (figure 1*a*,*b*); the cone is obtained by extending the incident ray in a straight line beyond its point of incidence on the rim, and rotating the extended part about the tangent to the rim (Keller 1962, figure 1*a*). A surprising fact is that the cone angle, i.e. the 'Keller angle' between the tangent and any ray on the cone, does not depend on the radial order s: by trigonometry from figure 2(*a*,*b*), its cosine is $\sin\theta_{ms}\sin\phi_{ms}$, i.e. m/ka, so that the angle may be denoted ψ_m. Hence

$$\cos\psi_m = \sin\theta_{ms}\sin\phi_{ms} = \frac{m}{ka}, \tag{2.35}$$

in accord with (2.6) and (2.12*a*). The relative orientations of the directions (θ_{ms}, ϕ_{ms}) on the cone are shown in figure 1(*a*,*b*): the orientations are determined by intersections of the cone with planes tilted at angles $\phi_{m1}, \phi_{m2}, \ldots, \phi_{ms_m}$ to the meridional plane through

the vertex of cone. In modelling the acoustics of aeroengines, it is often convenient to consider together all the propagating modes corresponding to a given frequency ω and circumferential order m; the 'swinging around' of their ray directions on a cone of fixed angle (figure 1*a*,*b*), and hence the general similarity of the radiation patterns for different s at fixed m, is thus of great interest for the 'source modelling' part of aeroengine noise research.

A different method of obtaining the cone angle is as follows. On the rim of the duct the phase varies as $\omega t - m\phi$, corresponding to a phase Mach number $a\omega/mc$, i.e. ka/m. Now a ray can only be emitted in, or received from, directions for which the resolved component of phase velocity is exactly sonic; hence the cosine of the cone angle must equal m/ka. This argument explains why the cone angle does not depend on the radial order s; equally, it explains the relation (2.35) between the mode angles θ_{ms} and ϕ_{ms}.

A section of the cone by a plane through the end face of the duct (figure 2*a*) shows that the cone touches the sonic cylinder of radius r_m defined by (2.4*a*) and (2.5*a*). This too may be explained by a phase argument: the circumferential phase Mach number at radius r_m is a fraction r_m/a of its value ka/m at the rim, i.e. the circumferential phase Mach number is 1, by (2.9*a*); hence the tangency of the cone and sonic cylinder is consistent with a wave travelling on the cone, away from the vertex, at the speed of sound. The plane section in figure 2(*a*) also shows the tangency of the incident ray and caustic surface $r = r_{ms}$; the ray is of course tilted at an angle θ_{ms} to the plane of the figure.

One quarter of the rays on the cone, forming a sector of 90° about the tangent to the rim, point back into the duct and generate the reflected field. The 90° spread of angles distributes the reflected field among many modes, and is a factor in determining the coupling coefficients, which quantify the conversion of one mode into another on reflection. The division of the rays into those pointing out of the duct and those pointing back into it corresponds to the 'energy budget' relation which equates the incident intensity to the sum of transmitted and reflected intensities. Rays pointing back into the duct are no different in kind from those pointing out, although they reflect off the walls of the duct to form piecewise linear helices, instead of propagating unimpeded in straight lines to the far field. Hence the reflected field is similar in many respects to the rearward-radiated field.

A section of the cone by a plane through its vertex and tangential to the duct wall (figure 2*b*) shows that the most forward-pointing ray on the cone makes an angle $\pi/2 - \psi_m$, i.e. θ_m, with the forward direction Ox; and the most rearward-pointing ray makes an angle θ_m with the backward direction. If the vertex of the cone is given every position on the rim, the resulting family of cones envelops two surfaces, which in the far field tend to cones of angle θ_m centred on the forward and backward directions of the duct axis. No ray can reach inside these two cones, which thus bound 'quiet zones', in which the field is exponentially small; therefore θ_m is the 'quiet-zone angle'. Outside of these two cones, each point in the far field is struck by at least one ray; the region outside the two cones is therefore the 'loud zone'. A remarkable feature of this division of space into quiet and loud zones is its fore-and-aft symmetry: in a problem with high-frequency sound propagating out of a duct, the structure of the field in the rear arc might not be expected to show any similarity to the structure in the forward direction. The symmetry would surely be quite mysterious without an explanation based on the Keller cones.

The far-field loud zone may be subdivided into the 'forward loud zone', ahead of the duct exit plane, and the 'backward loud zone', behind it. In the forward loud zone, two

rays pass through each point, from different points on the rim, and the interference of the field on the two families of rays will produce an oscillatory directivity pattern. In the backward loud zone, only one direct ray passes through each point, and the directivity pattern will not display rapid oscillations. This structure is precisely that which appears in a set of graphs computed by Homicz & Lordi (1975, figure 2) from the Wiener–Hopf solution for $m = 40$, $s = 3$ and $ka = 55, 70, 85$. Moreover, at the quiet-zone angles $\theta_{40} = \sin^{-1}(40/ka)$, namely 46.7°, 34.9°, 28.0°, the field in these graphs decays very sharply to zero, both in the fore and aft directions. The graphs therefore provide a striking confirmation of the ray theory.

An appealing physical description of the effect of the end of the duct is that it acts as a 'ring source' (cf. Prentice 1992); in optical terminology, it 'glows' under the influence of its irradiation from inside the duct. The glow is of course highly directional, and the division of the far field into different regions corresponds to the number of 'bright spots' seen on the rim by the observer.

The cones described above consist of singly diffracted rays, since they are produced by the incident field striking the rim of the duct. Some of these rays, namely those lying in the duct exit plane and pointing inwards, strike the rim again, to produce further cones; these are the cones of doubly diffracted rays. The process continues indefinitely, to give cones of the multiply diffracted rays (Keller 1958). All these cones have the same cone angle, because a ray from one part of the rim to another has the same angle to the tangent at each end (figure 2*a*). Hence inclusion of any number of these rays does not alter the number of points (0, 1, or 2) on the rim which send rays to any given observation point: each point simply contributes an infinite series. The greater the value of ka, the more rapidly the higher terms in the series decay: in many problems, the first term in the series will give ample accuracy for most directions. Such series occur in the asymptotic analysis of Wiener–Hopf solutions, for example in the asymptotic series for the 'universal function' of Weinstein (1969, appendix B).

When $m = 0$, the mode does not spin: except for the special case of a plane wave propagating in the axial direction, each ray zig-zags in a meridional plane by successive reflections off the duct wall. The entire field is obtained from a typical ray (figure 1*g*,*h*) by giving it every possible axial translation and rotation; thus the cylindrical caustic found earlier degenerates to a straight line, namely the duct axis, and the cones become flattened into 'discs of infinite radius', forming meridional planes. Hence the ray structure is similar to that of a two-dimensional parallel-plate duct (figure 1*i*,*j*).

In previous work on sound radiation from aeroengine ducts, the problem has occasionally been simplified either by modelling the duct as two-dimensional (e.g. Candel 1973; Boyd *et al.* 1984), or by assuming that $m^2 \ll ka$ (Rice 1978). This inequality implies that the caustic radius is negligibly small, so that the rays lie approximately in meridional planes (figure 1*g*,*h*). Comparison of figure 1(*a*,*b*) with figure 1(*g*,*h*) shows that the simplified models do not account correctly for the cones: they send diffracted rays in all polar directions, whereas models with correctly angled cones do not send rays into the quiet zones. Therefore the simplified models are not well-suited to determining the radiation from aeroengine ducts; and the same is true of the asymptotic results of Weinstein (1969) for two-dimensional ducts (pp. 161–166), for non-spinning modes (pp. 166–170), and in the $m^2 \ll ka$ limit (pp. 170–174). The great advantage of Debye's approximation over the 'large argument' approximation $m^2 \ll ka$ is that it respects the ray structure of the field. If diffraction theory is to be

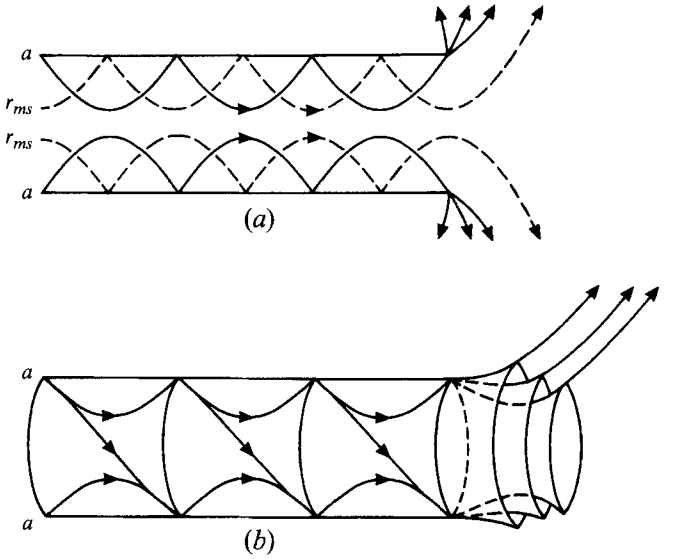

FIGURE 4. Cargill's meridional rays, and their diffraction at the end of the duct. (*a*) Hyperbolic arcs, incident and diffracted. (*b*) Hyperboloids generated either by rotation of (*a*), or by rotation of a piecewise linear helix.

applied to noise shielding by ducts, the angle of the cones is the most important thing to get right.

2.5. *Cargill's meridional rays*

A point of view emphasized by Cargill (1987, 1989) is that if a term $e^{-i(\omega t - m\phi)}$ is factored out of the pressure field, then ray theory may be applied directly to the resulting 'meridional wave equation' in the variables (r, x), without extraction of a Bessel function. The propagation speed in this equation depends on r, so that the rays are refracted onto curved arcs and are reflected off the duct walls before being diffracted at the end of the duct (figure 4*a*). Axial translations of a ray produce a caustic at a certain radius.

Cargill's approach based on the meridional wave equation is entirely equivalent to the three-dimensional approach adopted in this paper. For example, the meridional rays are meridional projections of the piecewise linear helices found earlier, and so form arcs of hyperbolae; this may be shown algebraically, but it also follows from the 'ruled surface' structure of a hyperboloid of one sheet (Hilbert & Cohn-Vossen 1952, figure 17), which shows that a hyperboloid may be generated from a pair of skew lines by rotating one of the lines about the other. The axial rotations of a meridional ray therefore produce the same surface as the axial rotations of a piecewise linear helical ray, namely the 'fish-net' shown in figure 4(*b*). Silent zones in a three-dimensional homogeneous medium correspond to geometrical shadow zones in a two-dimensional layered medium (Brekhovskikh 1980, figure 54.1); a ring source at the end of the duct (figure 4*b*) corresponds to a point source in a meridional plane (figure 4*a*). The smooth helices forming the rays in the inner cylinder in the three-dimensional theory project meridionally onto straight lines parallel to the duct axis in a meridional plane. Although a meridional theory of duct acoustics would be entirely tractable, using the armoury of techniques described by Brekhovskikh (1980), it seems easier to work

with straight lines and a uniform sound speed in three dimensions than hyperbolae and a non-uniform sound speed in two.

3. Conclusions and further work

The ray structure obtained in this paper establishes that the sound field radiated from the end of a cylindrical duct is similar to that radiated from a curved edge when it is struck by an incoming acoustic field. The curved edge in question is the rim of the end-face of the duct and the incoming acoustic field is a sum of infinite-duct modes. Except when the frequency of the incoming field is too low, the edge produces Keller cones of diffracted rays. Accurate numerical approximation to the the radiated field may therefore be obtained by the standard asymptotic techniques of Keller's geometrical theory of diffraction: the basic ingedient in this theory is the diffraction coefficient obtained from the exact solution of a 'canonical problem' with similar local geometry. Application of this technique to the cylindrical duct problem will require a moderate, but not excessive, amount of algebraic calculation, in which two familiar difficulties will need to be overcome. The first is that the canonical diffraction coefficients, when calculated in the most straightforward way, are singular in certain 'caustic' directions; the field in the neighbourhood of these directions requires a more complicated, but well-understood, uniform analysis. The second difficulty is that multiple reflections may, in certain directions, give the radiated field as a sum of terms which decay rather slowly; in these directions, comparison with the asymptotic limit of the Wiener–Hopf solution would be desirable. The asymptotic limit requires Weinstein's 'universal function'; the relation of this function to multiply-reflected rays is discussed in Bowman, Senior & Uslenghi (1987, pp. 46, 47).

More generally, a detailed comparison of the Keller-theory far-field radiation in all directions with that obtained from the Weiner–Hopf solution would be of great interest. Because of the curvature of the duct rim, the Keller cones have an envelope; this envelope, a caustic of the rays, extends from near the rim outwards to the far field and also backwards inside the duct. Comparison of the Keller and Wiener-Hopf results would therefore provide a check of the accuracy of Keller's method in a situation of non-trivial caustic geometry; the comparison would also determine when higher-order terms would be useful, or even essential, in the ray expansion of the field in inverse powers of the wavenumber. It would also be of interest to compare the far-field directivities obtained from both the Keller and Wiener–Hopf methods with those obtained from Kirchhoff's approximation (see the references in §1); the numerical evidence in Weinstein (1969) suggests that in many directions a suitable version of Kirchhoff's approximation would give excellent accuracy. The appeal of Kirchhoff's approximation in day-to-day engineering calculations is so great that one would often wish to use it right up to the limit of its range of validity. The results from all three methods could also be compared with those obtained from full-scale numerical computation (Myers & Lan 1993).

Realistic modelling of aeroengine ducts requires the incorporation of several effects not included in the simple model analysed in this paper. Effects which may readily be modelled by the Keller ray theory include (*a*) mean flow; (*b*) diffraction at bell-mouthed and scarfed inlets (Cargill 1989); (*c*) diffraction of the rearward propagating acoustic field in the duct when this field reaches the exhaust nozzle (Cargill 1982); and (*d*) arbitrary impedance of the duct lining (Rawlins 1978). Extension to cut-off modes is also feasible. For a complete prediction scheme, the theory needs to be

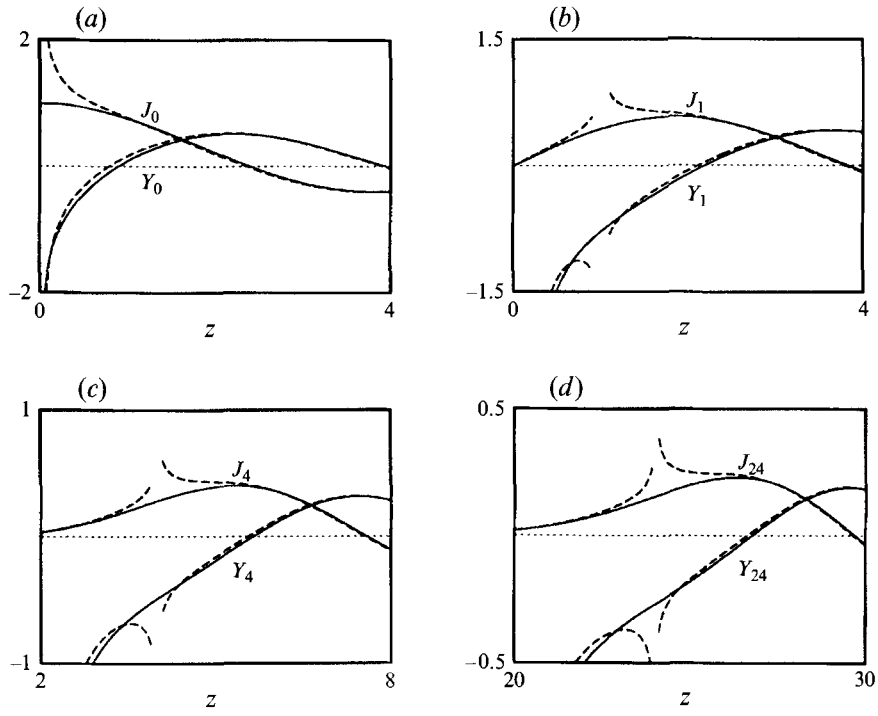

FIGURE 5. Bessel functions $J_m(z)$ and $Y_m(z)$ for $m = 0, 1, 4, 24$: —, exact; - - -, Debye approximation. The approximations are singular at the caustic value $z = m$. Note that the range $z > 0$ in graph (*a*), for $m = 0$, corresponds to just the right-hand sides $z > m$ of graphs (*b*)–(*d*), for $m = 1, 4, 24$; hence the shapes of all the graphs are similar.

combined with a model of the sources of sound in the duct; this problem is tackled in the sequel, Part 2 (Chapman 1995).

This work has been carried out with the support of the DTI (CARAD) through the Defence Research Agency, Pyestock. The author is grateful to A.B. Parry, S.J. Perkins, and other members of the aeroacoustics group at Rolls–Royce, Derby, for their comments and assistance at all stages of the project.

Appendix

Figure 5 consists of graphs of the Bessel functions $J_m(z)$ and $Y_m(z)$, and their Debye approximations, for $m = 0, 1, 4, 24$. The remarkable feature of these graphs is their almost identical shape: for any m, the approximation fails only in the last 'quarter wavelength', of order $m^{1/3}$, on either side of the caustic value $z = m$. Further details of the matching of Debye's approximation with an Airy function expression may be found in Crighton & Parry (1992). To obtain Debye's approximation for $m = 0$, it is necessary to put $\beta = \pi/2 - m/z$ in the expressions for $J_m(m \sec \beta)$ and $Y_m(m \sec \beta)$ given in Abramowitz & Stegun (1965, §9.3.3), and let $m \to 0$; the result is the large-argument, fixed-order 'Hankel type' asymptotic form for $m = 0$ (Abramowitz & Stegun 1965, §§9.2.1, 9.2.2). Thus Debye's approximation and Hankel's approximation are identical for $m = 0$.

REFERENCES

ABRAMOWITZ, M. & STEGUN, I. A. 1965 *Handbook of Mathematical Functions.* Dover.

BAXTER, S. M. & MORFEY, C. L. 1986 *Angular Distribution Analysis in Acoustics.* Lecture Notes in Engineering, Vol. **17**. Springer.

BOYD, W. K., KEMPTON, A. J. & MORFEY, C. L. 1984 Ray–theory predictions of the noise radiated from aeroengine ducts. *AIAA Paper* 84–2332.

BOWMAN, J. J., SENIOR, T. B. A. & USLENGHI, P. L. E. (EDS.) 1987 *Electromagnetic and Acoustic Scattering from Simple Shapes.* Harper & Row.

BREKHOVSKIKH, L. M. 1980 *Waves in layered media* (2nd edn). Academic.

BROADBENT, E. G. 1977 Noise shielding for aircraft. *Prog. Aerospace Sci.* **17**, 231–268.

CANDEL, S. M. 1973 Acoustic radiation from the end of a two–dimensional duct, effects of uniform flow and duct lining. *J. Sound Vib.* **28**, 1–13.

CARGILL, A. M. 1982 The radiation of high frequency sound out of a jet pipe. *J. Sound Vib.* **83**, 313–337.

CARGILL, A. M. 1987 A note on high frequency duct radiation. *Internal report, Rolls–Royce, Derby, England.*

CARGILL, A. M. 1989 Kirchhoff diffraction theory applied to a bell–mouthed duct. *Internal report, Rolls–Royce, Derby, England.*

CHAPMAN, C. J. 1995 Sound radiation from a cylindrical duct. Part 2. *J. Fluid Mech.* (submitted).

CHOUDHARY, S. & FELSEN, L. B. 1974 Analysis of Gaussian beam propagation and diffraction by inhomogeneous wave tracking. *Proc. IEEE* **62**, 1530–1541.

CRIGHTON, D. G. & PARRY, A. B. 1992 Higher approximations in the asymptotic theory of propeller noise. *AIAA J.* **30**, 23–28.

EVERSMAN, W. 1991 Theoretical models for duct acoustic propagation and radiation. In *Aeroacoustics of Flight Vehicles: Theory and Practice, Volume 2: Noise Control* (ed. H.H. Hubbard), pp. 101–163. NASA reference publication 1258, vol. 2.

FELSEN, L. B. 1984 Progressing and oscillatory waves for hybrid synthesis of source excited propagation and diffraction. *IEEE Trans. Antennas and Propagation* **AP–32**, 775–796.

FELSEN, L. B. & YEE, H. Y. 1968 Ray method for sound-wave reflection in an open-ended circular pipe. *J. Acoust. Soc. Am.* **44**, 1028–1039.

GOLDSTEIN, M. E. 1976 *Aeroacoustics.* McGraw–Hill.

HILBERT, D. & COHN-VOSSEN, S. 1952 *Geometry and the Imagination.* Chelsea.

HOMICZ, G. F. & LORDI, J. A. 1975 A note on the radiative directivity patterns of duct acoustic modes. *J. Sound Vib.* **41**, 283–290.

JONES, D. S. 1977 The mathematical theory of noise shielding. *Prog. Aerospace Sci.* **17**, 149–229.

KELLER, J. B. 1958 A geometrical theory of diffraction. *Proc. Symp. Appl. Math.* **8**, 27–52.

KELLER, J. B. 1962 Geometrical theory of diffraction. *J. Optical Soc. Am.* **52**, 116–130.

KELLER, J. B. & RUBINOW, S. I. 1960 Asymptotic solution of eigenvalue problems. *Ann. Physics* **9**, 24–75.

KINBER, B. YE. 1962 Diffraction at the open end of a sectoral horn. *Radio Engng Electron. Phys.* **7**, 1620–1632.

KRAVTSOV, YU. A. 1967 Complex rays and complex caustics. *Izv. VUZ Radiofiz.* **10**, 1283–1304. (Translated in *Radiophysics and Quantum Electronics* **10**, 719–730, 1971.)

LANSING, D. L. 1970 Exact solution for radiation of sound from a semi–infinite circular duct with application to fan and compressor noise. In *Analytical Methods in Aircraft Aerodynamics,* pp. 323–334. NASA SP–228.

LEVINE, H. & SCHWINGER, J. 1948 On the radiation of sound from an unflanged circular pipe. *Phys. Rev.* **73**, 383–406.

MORFEY, C. L. 1969 A note on the radiation efficiency of acoustic duct modes. *J. Sound Vib.* **9**, 367–372.

MORFEY, C. L., SHARLAND, I. J. & YEOW, K. W. 1968 Fan noise. In *Noise and Acoustic Fatigue in Aeronautics* (ed. E.J. Richards & D.J. Mead), pp. 215–240. Wiley.

MYERS, M. K. & LAN, J. H. 1993 Sound radiation from ducted rotating sources in uniform motion. *AIAA Paper* 93–4429.

PRENTICE, P. R. 1992 The acoustic ring source and its application to propeller acoustics. *Proc. R. Soc. Lond.* A **437**, 629–644.

RAWLINS, A. D. 1978 Radiation of sound from an unflanged rigid cylindrical duct with an acoustically absorbing internal surface. *Proc. R. Soc. Lond.* A **361**, 65–91.

RICE, E. J. 1978 Multimodal far-field acoustic radiation pattern using mode cutoff ratio. *AIAA J.* **16**, 906–911.

RICE, E. J., HEIDMANN, M. F. & SOFRIN, T. G. 1979 Modal propagation angles in a cylindrical duct with flow and their relation to sound radiation. *AIAA Paper* 79–0183.

TYLER, J. M. & SOFRIN, T. G. 1962 Axial flow compressor noise studies. *Trans. Soc. Automotive Engrs* **70**, 309–332.

WANG, W.-Y. D. & DESCHAMPS, G. A. 1974 Application of complex ray tracing to scattering problems. *Proc. IEEE* **62**, 1541–1551.

WEINSTEIN, L. A. 1949 The theory of sound waves in open tubes [in Russian]. *Zh. Tech. Fiz.* **19**, 911–930.

WEINSTEIN, L. A. 1969 *The Theory of Diffraction and the Factorization Method (Generalized Wiener–Hopf technique)*. Golem.

WRIGHT, S. E. 1972 Waveguides and rotating sources. *J. Sound Vib.* **25**, 163–178.

YEE, H. Y., FELSEN, L. B. & KELLER, J. B. 1968 Ray theory of reflection from the open end of a waveguide. *SIAM J. Appl. Maths* **16**, 268–300.